A Quasioptical Vector Interferometer for Polarization Control

David T. Chuss, Edward J. Wollack, S. Harvey Moseley

NASA Goddard Space Flight Center
Greenbelt, MD 20771

David.T.Chuss@nasa.gov

Giles Novak

Department of Physics and Astronomy, Northwestern University
2145 Sheridan Road, Evanston, IL 60208

We present a mathematical description of a Quasioptical Vector Interferometer (QVI), a device that maps an input polarization state to an output polarization state by introducing a phase delay between two linear orthogonal components of the input polarization. The advantages of such a device over a spinning wavelplate modulator for measuring astronomical polarization in the far-infrared through millimeter are: 1. The use of small, linear motions elimates the need for cryogenic rotational bearings, 2. The phase flexibility allows measurement of Stokes V as well as Q and U, and 3. The QVI allows for both multi-wavelength and broadband modulation. We suggest two implementations of this device as an astronomical polarization modulator. The first involves two such modulators placed in series. By adjusting the two phase delays, it is possible to use such a modulator to measure Stokes Q, U, and V for passbands that are not too large. Conversely, a single QVI may be used to measure Q and V independent of frequency. In this implementation, Stokes U must be measured by rotating the instrument. We conclude this paper by presenting initial laboratory results. © 2005 Optical Society of America

OCIS codes: 000.0000, 999.9999.

1. Introduction

Astronomical polarimetry is currently drawing much attention, mostly due to the anticipated high-sensitivity searches for the so-called "B-modes" of the Cosmic Microwave Background Polarization. These signatures of gravitational waves produced during the inflationary epoch will provide a direct measurement of the energy scale of inflation. The amplitude of the B-modes is theorized to be 10^{-7} to 10^{-9} of the power of the CMB, and so its measurement will require a good modulation strategy and an unprecedented control of systematics.

The emission from magnetically-aligned dust in our Galaxy provides a contaminant that will have to be understood in order to correctly extract the B-modes from the total signal. On the other hand, this polarized emission provides a tool for analyzing the role of magnetic fields in star formation, and with the advent of multi-wavelength submillimeter and far-infrared photometers such as SCUBA2[1] and HAWC/SOFIA,[2] there is an opportunity to expand this field of study. To take advantage of the new detector technology that will be coming online in the next few years, it is necessary to develop the polarization modulation technology that will enable the conversion of these photometers into polarimeters.

Fundamentally, polarization arises as a result of statistical correlations between the electric field components in the plane perpendicular to the propagation direction. These correlations are represented by complex quantities, and so in the measurement of polarized light, it is convenient to use real linear combinations of these correlations, namely, the Stokes parameters, I, Q, U, and V.

It is possible to trace the polarization state of radiation through a quasioptical system by determining the transformations describing the mapping of the input to output polarization states. We are specifically concerned with the class of optical elements for which Stokes I is decoupled from the other Stokes parameters. For this class of elements, the polarization,

$$P^2 = Q^2 + U^2 + V^2 \tag{1}$$

is constant. This equation can be interpreted to describe the points on the surface of a sphere in a three dimensional space having Q, U, and V as its coordinate axes. This sphere is known as the Poincaré sphere, and the action of any given ideal polarization modulator can be represented by a rotation (and possibly an inversion) in this space. Such an operation corresponds to the introduction of a phase delay between orthogonal polarizations, which is the physical mechanism at work in a polarization modulator. The two free parameters in any given transformation are the basis in which the phase delay is introduced and the magnitude of the phase delay itself. These two parameters directly define the orientation and the magnitude of the rotation on the Poincarë sphere: the rotation axis is defined by the sphere diameter connecting the two polarization states between which the phase is introduced, and the magnitude of the rotation is equal to that of the introduced phase.[3]

In order to measure the polarized part of a partially-polarized signal, it is desirable to separate the polarized part of the signal from the unpolarized part. This is especially crucial when the fractional polarization of the signal is small. One way to do this is to methodically change, or modulate, the polarized part of the signal (by changing one of the parameters of the polarization modulator) while leaving the unpolarized part unaffected. Periodic rotations in Poincaré space can accomplish this encoding of the polarized component of the signal for subsequent synchronous demodulation and detection. A convenient way of formulating the problem is to envision a detector that is sensitive to Stokes Q when projected onto the sky in the absence of modulation. The polarization modulator then systematically changes the polarization state to which the detector is sensitive such that the polarization state of the light can be completely characterized.

A common implementation of such a polarization modulator is a dielectric birefringent plate.[4] A birefringent plate consists of a piece of birefringent material cut so as to delay one linear polarization component relative to the other by the desired amount (generally either to one-half or one-quarter of the wavelength of interest). In this case, the phase difference is fixed and the modulation is accomplished by physically rotating the birefringent plate.

In contrast, we introduce a polarization modulator that hold the basis of phase introduction contant and modulates the polarization by changing the magnitude of the phase difference. This Quasioptical Vector Interferometer (QVI) can be thought of as a Martin-Puplett interferometer with the input polarizer removed. The relative phase between orthogonal linear polarizations can be adjusted by adjusting their physical path lengths. This type of device has features in common with the back end of a polarimeter that uses a Fresnel Romb and a Martin-Puplett interferometer in series.[5] Here, we describe two astronomical polarimeter architectures that employ QVIs to measure linear polarization.

The first implementation involves two QVIs placed in series. In this case, we are assuming a narrow enough passband such that the phase delays introduced for the center wavelength approximately apply to the whole band. The QVIs are configured as follows: the QVI that is closest to the polarization-sensitive detector has its beam-spliting grid oriented at an angle of 45° with respect to the axis of the detector (Q-axis; see above), and the other interferometer has its grid oriented at 22.5° with respect to the detector axes. We show how full modulation of all linear and circular polarization states can be achieved with this device. The use of this architecture in a polarimeter that measures linear polarization can be understood as follows: If we set the interferometer closest to the source (interferometer 1) for zero phase delay, and switch the interferometer closest to the detector (interferometer 2) between delays of 0 and π, then the detector axes, as projected onto the plane of the sky, will switch between Q and $-Q$. With interferometer 1 set to a phase delay of π, switching interferometer 2 between 0 and π will project the detector axes to $\pm U$. The dual QVIs provide two degrees of freedom,

namely the phase delays for each interferometer. The angles selected for the two basis sets are those for which the two degrees of freedom correspond to orthogonal coordinates on the Poincaré sphere, thus allowing all polarization states to be accessible to the detector.

For passbands for which the above approximation fails, one can use a single QVI to measure Stokes Q and V as a function of frequency across the band by taking the Fourier transform of the path difference. This technique is inherently frequency-independent. However, in order to measure Stokes U, the instrument needs to be rotated by 45°.

There are several qualities that make this architecture a viable candidate technology for future astronomical polarimeters operating in the far-infrared through millimeter parts of the spectrum. First, whereas a given birefringent plate can be built to measure either circular or linear polarization but not both, the Martin-Puplett architecture allows for designs that cover the entire Poincaré sphere. Second, since the path difference between orthogonal linear polarization states is variable, these devices are easily retuned for use at multiple wavelengths. Note also, that since the QVI is used in reflection, frequency-dependent antireflective coatings are not required. Finally, this architecture requires only small linear translations that will eliminate the need for complicated systems of shafts, gears, and bearings that are common in birefringent plate modulators.[6] All of these qualities are beneficial to the future effort to measure the polarized flux of astronomical and cosmological sources from space-borne telescopes.

Our frequency-dependent analysis will require the use of Jones, Density, and Müller matrices, so we begin with a review of these methods (section 2). In section 3, we derive the Müller matrix representation of the Martin-Pupplett interferometer. Using this result, we calculate the frequency dependent performance of a QVI in section 4. Section 5 describes various applications of the modulator, and section 6 gives the results of laboratory tests of the polarization-modulating properties of a single QVI.

2. Polarization Matrix Methods

In this section, we review the properties of Jones, Density, and Müller matrices and their relationships which enable analysis of the QVI.

2.A. Jones Matrices

Jones matrices[7] are a convenient way to analyze radiation as it propagates through an optical system in architectures in which it is important to keep track of phase. For the ideal case, we assume that all ports are matched and so no cavities are formed. These two conditions apply to the QVI when used in an astronomical instrument. This formulation is applicable for coherent radiation; however, it can be extended using using the closely-related formalism of density matrices to treat the problem of partially polarized light.[8]

4

Jones Matrices are 2×2 matrices that contain information about how the orthogonal electric field components transform in an optical system. The input Jones vector is defined as follows:

$$|E\rangle = \begin{pmatrix} E_x \\ E_y \end{pmatrix} \equiv \begin{pmatrix} E_H \\ E_V \end{pmatrix} \tag{2}$$

The output vector from an optical system can then be represented by $|E_f\rangle = \bar{J}|E_i\rangle$ where $\bar{J}$ is the vector transformation introduced by the optical system. The power measured at a detector at the back end of such a system is given by

$$\langle E_f|\bar{J}_{det}|E_f\rangle = \langle E_i|\bar{J}^\dagger \bar{J}_{det}\bar{J}|E_i\rangle. \tag{3}$$

The matrix $\bar{J}_{det}$ is dependent on the properties of the detector used to make the measurement.

In the Jones matrix representation, Stokes parameters are represented by the Pauli matrices and the identity matrix.

$$\bar{I} \equiv \bar{\sigma}_0 = \begin{pmatrix} 1 & 0 \\ 0 & 1 \end{pmatrix}, \bar{Q} \equiv \bar{\sigma}_1 = \begin{pmatrix} 1 & 0 \\ 0 & -1 \end{pmatrix}, \bar{U} \equiv \bar{\sigma}_2 = \begin{pmatrix} 0 & 1 \\ 1 & 0 \end{pmatrix}, \bar{V} \equiv \bar{\sigma}_3 = \begin{pmatrix} 0 & -i \\ i & 0 \end{pmatrix} \tag{4}$$

In using the Jones matrix formalism in this paper, we will use the convention that a bar over the Stokes symbol indicates its Jones matrix representation. An un-barred Stokes parameter represents measurable power (e.g. $Q = \langle E|\bar{Q}|E\rangle$). Note that the measured power in each of the Stokes parameters are

$$I = \langle E|\bar{I}|E\rangle = E_H^2 + E_V^2 \tag{5}$$

$$Q = \langle E|\bar{Q}|E\rangle = E_H^2 - E_V^2 \tag{6}$$

$$U = \langle E|\bar{U}|E\rangle = 2\Re(E_H^* E_V) \tag{7}$$

$$V = \langle E|\bar{V}|E\rangle = 2\Im(E_H^* E_V) \tag{8}$$

$$\tag{9}$$

These equation connect the Jones matrix formulation of the Stokes parameters to their familiar definitions.[9,3]

These four Stokes matrices have the following multiplicative properties. Defining $(\bar{\sigma}_0, \bar{\sigma}_1, \bar{\sigma}_2, \bar{\sigma}_3) \equiv (\bar{I}, \bar{Q}, \bar{U}, \bar{V})$, $\bar{\sigma}_0 \bar{\sigma}_\alpha = \bar{\sigma}_\alpha \bar{\sigma}_0 = \bar{\sigma}_\alpha$ for $\alpha \in (0, 1, 2, 3)$ and $\bar{\sigma}_j \bar{\sigma}_k = \sum_l \epsilon_{jkl} i \bar{\sigma}_l + \delta_{jk} \bar{\sigma}_0$ for $j, k, l \in (1, 2, 3)$. These four matrices form a convenient basis for expressing Jones matrices. Table 1 shows both the explicit Jones matrices and the Stokes expansion for selected optical transformations. The mirror transformation, which can be expressed simply as $\bar{Q}$, sets the convention for how the $(\hat{H}, \hat{V})$ coordinate system is propagated through the optical system. Note that for some structures, the Stokes expansion provides a convenient way to express optical elements. Successive transformations can be calculated either by matrix algebra or by the Pauli algebra defined above.

5

2.B. Density Matrices

In the general case of partially polarized light, polarization arizes because of time-averaged (statistical) correlations between the electric field components. The density matrix is a complex 2×2 matrix that fully characterizes the polarization state of the light. It is given by

$$\bar{D} = \begin{pmatrix} \langle E_x^* E_x \rangle & \langle E_x^* E_y \rangle \\ \langle E_y^* E_x \rangle & \langle E_y^* E_y \rangle \end{pmatrix}. \tag{10}$$

Here, the brackets indicate a time average. If the density matrix is expressed as a linear combination of the Pauli matrices, $\bar{D} = I\bar{\sigma}_0 + Q\bar{\sigma}_1 + U\bar{\sigma}_2 + V\bar{\sigma}_3$, the coefficients are the Stokes parameters.

The transformation of the polarization state by an optical system is given by a similarity transformation, $\bar{D}' = \bar{J}^\dagger \bar{D} \bar{J}$. Here, $\bar{J}$ is the Jones matrix describing the optical system. For the purposes of this paper, we are interested in how the polarization state of the detectors map onto the sky, and so $\bar{D}_{sky} = \bar{J}^\dagger \bar{D}_{det} \bar{J}$. Note the similarity in the transformation of the density matrix and the expression for total power in the Jones matrix formalism (Equation 3).

2.C. Müller Matrices

Until now, no limitations have been placed on $\bar{J}$, the matrix describing an optical system under consideration. If the magnitude of the determinant of $\bar{J}$ is unity, then there is a homomorphism between the group of 2×2 matrices having $|det(\bar{J})| = 1$ and the Poincaré or Inhomogenous Lorentz group. In this case, the quantity $I^2 - Q^2 - U^2 - V^2$ is preserved under these transformations. In analogy to special relativity,[11] the inhomogeneous Lorentz group can be represented by a group of 4×4 real matrices acting on a Stokes vector, $\bar{S} = (I, Q, U, V)$. These matrices are known as Müller matrices. For our purposes, we consider the Müller matrix that maps the Stokes parameters at the detector to the sky: $\bar{S}_{sky} = \bar{M} \bar{S}_{det}$.

For polarization modulation, we are particularly interested in the case for which the Jones matrices describing our optical system are unitary. In this case, Stokes I decouples from the other Stokes parameters and the quantity $P^2 = Q^2 + U^2 + V^2$ is preserved. This subgroup can be represented by 3 × 3 orthogonal submatrices that represent symmetries on the surface of a sphere in a space having Stokes Q, U, and V as axes. This sphere is called the Poincaré sphere.

As an aside we note that if we restrict the group of Density matrices to those with positive determinants, the system is described by SU(2), and thus there is a homomorphism between this group and SO(3) the group of rotations on the Poincaré sphere. These are the groups that are important to a wave plate; however, the physical reflection involved in the QVI architecture introduces a negative determinant, resulting in combinations of rotations and reflections on the Poincaré sphere.

6

3. Martin-Puplett Interferometer

As an example of a QVI, we specifically consider the case of the Martin-Puplett interferometer with the input polarized removed and propagate the polarization through the architecture using the formalisms described above. Here, we start with a Jones matrix and use this description to calculate the elements of the corresponding Müller matrix.

A diagram of a Martin-Puplett Interferometer is shown in Figure 1. Light enters from the left and is split into two orthogonal polarizations by the 45° grid. The two components of polarization are then sent to two roof top mirrors which rotate the polarization by 90° with respect to the grid wires. The beams recombine at the beam splitter and exit the device at the top.

We will examine this device using Jones matrices, labeling the angle of the device to be the angle of the beam-splitting grid as seen by the incoming radiation. We will first look at the case of an interferometer at a rotation of 45° and then generalize to an arbitrary angle using a similarity transformation. For the simple case, the Jones matrix representing this configuration, $\bar{J}_{MP}(\pi/4)$, can be expressed as the sum of the Jones matrices for the radiation in each of the arms of the interferometer.

$$\bar{J}_{MP}\left(\frac{\pi}{4}\right) = \bar{J}_{MP}^{(1)}\left(\frac{\pi}{4}\right) + \bar{J}_{MP}^{(2)}\left(\frac{\pi}{4}\right) \tag{11}$$

In turn, each of these terms can be decomposed into a product of the Jones matrices of the individual elements in each optical path. The Jones matrices for these elements are given in Table 1.

$$\bar{J}_{MP}^{(1)}\left(\frac{\pi}{4}\right) = \bar{J}_{WT}\left(\frac{\pi}{4}\right)\bar{J}_z(d_1)\bar{J}_{RT}(0)\bar{J}_z(d_1)\bar{J}_{WR}\left(\frac{\pi}{4}\right) = \begin{pmatrix} 1 & 1 \\ -1 & -1 \end{pmatrix}\frac{\exp(i4\pi d_1/\lambda)}{2} \tag{12}$$

$$\bar{J}_{MP}^{(2)}\left(\frac{\pi}{4}\right) = \bar{J}_{WR}\left(-\frac{\pi}{4}\right)\bar{J}_z(d_2)\bar{J}_{RT}(0)\bar{J}_z(d_2)\bar{J}_{WT}\left(\frac{\pi}{4}\right) = \begin{pmatrix} 1 & -1 \\ 1 & -1 \end{pmatrix}\frac{\exp(i4\pi d_2/\lambda)}{2} \tag{13}$$

Making the definition $\Delta \equiv 4\pi(d_2 - d_1)/\lambda$ and setting $\xi \equiv \Delta/2$, we arrive at the following.

$$\bar{J}_{MP}\left(\frac{\pi}{4}, \xi\right) = \frac{1}{2}e^{i2\pi(d_1+d_2)/\lambda}\begin{pmatrix} \cos\xi & -i\sin\xi \\ i\sin\xi & \cos\xi \end{pmatrix} \tag{14}$$

Next, we derive an expression for a Martin-Puplett interferometer placed at an arbitrary angle θ. Recall that the definition of θ we have chosen is the angle of the grid with respect to $\hat{H}$ for the radiation at the input port. To do this, we transform into the coordinate system for which we have already solved the problem, apply the transformation for $\bar{J}_{MP}(\pi/4)$, and then transform back. In the case of the Martin-Puplett interferometer, there is a subtlety. Because the Martin Puplett architecture involves an odd number of reflections, the angle of

the device as viewed from the outgoing light is the negative of that viewed from the incoming light. This reflection is accounted for in the similarity transformation. Setting $\chi = (\theta - \pi/4)$, we note that

$$\bar{J}_{MP}(\chi, \xi) = \bar{R}^\dagger(-\chi)\bar{J}_{MP}\left(\frac{\pi}{4}\right)\bar{R}(\chi)\frac{e^{i2\pi(d_1+d_2)/\lambda}}{2}\begin{pmatrix} \cos\xi + i\sin\xi\cos 2\chi & -i\sin\xi\cos 2\chi \\ i\sin\xi\cos 2\chi & -\cos\xi + i\sin\xi\sin 2\chi \end{pmatrix}$$

$$(15)$$

$$\bar{J}_{MP}(\theta, \xi) = e^{i2\pi(d_1+d_2)/\lambda}\begin{pmatrix} \cos\xi - i\sin\xi\cos 2\theta & -i\sin\xi\sin 2\theta \\ i\sin\xi\sin 2\theta & -\cos\xi - i\sin\xi\cos 2\theta \end{pmatrix} \quad (16)$$

In terms of the Stokes parameter basis set, this expression is

$$\bar{J}_{MP}(\theta, \xi) = e^{i2\pi(d_1+d_2)/\lambda}\left[\bar{Q}\cos\xi - i\sin\xi(\bar{I}\cos(2\theta) + i\bar{V}\sin(2\theta))\right] \quad (17)$$

Note that within a phase factor (which is irrelevant in a measurement of power) $\bar{J}_{MP} = \bar{Q}\bar{J}_{WP}$. This means that the action of the Martin-Puplett modulator is equivalent to that of a birefringent plate (a relative retardation between orthogonal linear polarization components) followed by a reflection (represented as the Jones matrix $\bar{Q}$).

The matrix in Equation 17 is unitary, and its determinant is -1. Thus its Müller representation is expected to describe symmetries on the Poincaré sphere. By expanding the density matrices in the Pauli matrix basis both before and after performing the similarity transform corresponding to the optical system, one can generate the Müller matrix for the system.

$$\bar{M}_{MP}(\theta, \Delta) = \begin{pmatrix} 1 & 0 & 0 & 0 \\ 0 & \cos^2 2\theta + \cos\Delta\sin^2 2\theta & -\sin 2\theta\cos 2\theta(1-\cos\Delta) & \sin 2\theta\sin\Delta \\ 0 & \sin 2\theta\cos 2\theta(1-\cos\Delta) & -\sin^2 2\theta - \cos\Delta\cos^2 2\theta & -\cos 2\theta\sin\Delta \\ 0 & \sin 2\theta\sin\Delta & \cos 2\theta\sin\Delta & -\cos\Delta \end{pmatrix}$$

$$(18)$$

This matrix can be expressed as a product of symmetry operations on the Poincaré sphere.

$$\bar{M}_{MP}(\theta, \Delta) = \bar{\Gamma}_{QV}\bar{\Gamma}_{QU}\bar{R}_V(2\theta)\bar{R}_Q(\Delta)\bar{R}_V(-2\theta) = \bar{\Gamma}_{QV}\bar{\Gamma}_{QU}\bar{M}_{WP}(\theta, \Delta) \quad (19)$$

Here, $\bar{\Gamma}_{QV}$ is a reflection about the $Q-V$ plane, $\bar{\Gamma}_{QU}$ is a reflection about the $Q-U$ plane, $\bar{R}_V$ is a rotation around the $V-$axis, and $\bar{R}_Q$ is a rotation around the $Q-$axis. The matrix $\bar{M}_{WP}(\theta, \Delta)$ is the Poincaré sphere transformation for a wave plate. This transformation is a rotation about an axis in the $Q-U$ plane oriented at an angle 2θ measured from Q towards U, where θ is the physical angle of the fast (or slow) axis of the wave plate.

4. Polarization Modulation

We assume that the detector at the back end of our optical system is sensitive to Stokes Q. This is essentially a statement about the orientation of the analyzer in the optical system.

Strictly speaking, a Q sensitive detector requires a differencing of two orthogonal linearly polarized detectors with an orientation that we choose to define the Q-axis. However, the following discussion also applies to the class of polarized detector strategies that only collect one linear polarization. Such detectors are technically sensitive to $Q \pm I$, but, to lowest order or in ideal modulation, I does not couple to the polarization modulation.

The modulator changes the polarization state of this detector as projected onto the sky. For a single Martin-Puplett modulator, the polarization state that the detector measured can be calculated from the second column of the Müller matrix.

$$Q_{det} = Q_{sky}(\cos^2 2\theta + \cos \Delta \sin^2 2\theta) + U_{sky} \sin 2\theta \cos 2\theta (1 - \cos \Delta) + V_{sky}(\sin 2\theta \sin \Delta) \quad (20)$$

For the Martin-Puplett architecture, θ is fixed and Δ is modulated. Using a single Martin-Puplett, it is not possible to completely modulate Q, U, and V. To see an example of this, consider the case, where θ is set to $\pi/4$. In this case,

$$Q_{det} = Q_{sky} \cos \Delta + V_{sky} \sin \Delta. \quad (21)$$

In Fourier transform spectrometer applications, a grid is placed in front of the mechanism so as to set the initial polarization to $Q(\lambda)$. The assumption here is that the light is approximately unpolarized such that $Q(\lambda) = \frac{1}{2} I(\lambda)$. Here, $I(\lambda)$ is the spectrum of the radiation. The power remaining in the Q polarization state at the output port of the interferometer will be a function of the incident spectrum and the wavelength-dependent phase delay introduced by the intereferometer.

$$Q'(\lambda, \delta) = Q(\lambda) \cos \Delta \quad (22)$$

where $\Delta = 4\pi\delta/\lambda$, and δ is the path difference. In this case, $Q(\lambda)$ is the spectrum of the incident radiation. A bolometric detector sensitive to Q will measure the integrated power as a function of path difference:

$$Q'(\delta) = \int_0^\infty Q(\lambda)\phi(\lambda) \cos \Delta d\lambda \quad (23)$$

Here, $\phi(\lambda)$ is a function describing the effective frequency response of the instrument.

Taking the Fourier transform, one finds that

$$Q(\lambda)\phi(\lambda) = \int_{\delta_1}^{\delta_2} Q'(\delta) e^{2\pi i\delta/\lambda'} d\delta \quad (24)$$

Here, δ_1 and δ_2 are the minimum and maximum path differences of the scan. upon calibration of the instrument's frequency response, the spectrum of the source is recovered. Thus, our analysis confirms that the Martin-Puplett interferometer can be used as an FTS with a 50% maximum efficiency.

On the other hand, in the absence of the initial polarizer, the interferometer will modulate the power of the source that is present in both the Q and V polarization states. For the case where $V = 0$, the Fourier transform will produce the spectral dependence of Stokes Q in the source. This particular modulation scheme is notable in that it is frequency-independent. The major drawback for this architecture is its insensitivity to Stokes U. For a space-borne experiment, U can be recovered by rotation of the spacecraft. For ground-based instruments, sufficient rotation is problematic, and thus an alternative approach may be required.

An alternative to instrument rotation is to place two such devices in series. It is possible to calculate the functional form of the polarization signal on the detectors by simply chaining the two Müller matrices together. The transfer equation of the optical system now looks like $\bar{S}_{sky} = \bar{M}_{MP}(\theta_1, \Delta_1)\bar{M}_{MP}(\theta_2, \Delta_2)\bar{S}_{det}$ Note that modulator 2 is closer to the detector than modulator 1. Because our detectors are sensitive to only Q, we solve the second column of the resulting matrix.

$$
\begin{aligned}
Q_{det} = Q_{sky}[&(\cos^2 2\theta_1 + \cos \Delta_1 \sin^2 2\theta_1)(\cos^2 2\theta_2 + \cos \Delta_2 \sin^2 2\theta_2) \\
&- \sin 2\theta_1 \cos 2\theta_1 \sin 2\theta_2 \cos 2\theta_2 (1 - \cos \Delta_1)(1 - \cos \Delta_2) \\
&+ \sin 2\theta_1 \sin 2\theta_2 \sin \Delta_1 \sin \Delta_2] \\
+ U_{sky}[&\sin 2\theta_1 \cos 2\theta_1 (1 - \cos \Delta_1)(\cos^2 2\theta_2 + \cos \Delta_2 \sin^2 2\theta_2) \\
&- (\cos^2 2\theta_1 + \cos \Delta_1 \sin^2 2\theta_1) \sin 2\theta_2 \cos 2\theta_2 (1 - \cos \Delta_2) \\
&- \cos 2\theta_1 \sin 2\theta_2 \sin \Delta_1 \sin \Delta_2] \\
+ V_{sky}[&\sin 2\theta_1 \sin \Delta_1 (\cos^2 2\theta_2 + \cos \Delta_2 \sin^2 2\theta_2) \\
&+ \cos 2\theta_1 \sin 2\theta_2 \cos 2\theta_2 \sin \Delta_1 (1 - \cos \Delta_2) \\
&- \sin 2\theta_2 \cos \Delta_1 \sin \Delta_2]
\end{aligned}
\tag{25}
$$

We now consider the specific case where $\theta_1 = \pi/8$ and $\theta_2 = \pi/4$. Polarized sensitivities for selected pairs of phase delay settings for the pair of modulators are shown in Table 2. It is possible to fully characterize the polarization state. The simplest method for doing this is adopt a single phase delay over the entire bandwidth. In this case, one sets the modulators to the desired detector polarization sensitivtiy and makes a measurement. One then repeats this measurement for each state and builds up information about the polarization state of the source.

One of the strengths of this modulator is its ability to modulate quickly between different polarization states. This has the advantage of putting the polarization signal above the $1/f$ knee of the instrument noise spectrum without having to resort to other modulation schemes such as chopping of the secondary or scanning the telescope.

It is also possible to extend the bandwidth in a way similar to the single modulator above. One could scan these modulators through a range of delays and extract the frequency-

dependent Stokes parameters.

5. Other Implementations

The Martin-Puplett architecture is not a unique implementation of a QVI. In fact there are several quasioptical arrangement of grids and mirrors that correspond to Jones matrices that differ only by an absolute phase from those that describe the Martin-Puplett. The simplest of these designs is a system consisting of a polarizing grid placed in front of a mirror. This design is similar in structure to a reflecting waveplate,[12] but in this case, modulation occurs by modulating the grid-mirror difference rather than by spinning the plate. This alternative design for a polarizing interferometer has been previously employed of its compact features and relative ease of construction.[13]

6. Systematics

In developing a polarization modulator, one must consider the possibility of instrumental effects introduced by the action of the modulation. In a dielectric half-wave plate, such an effect arises from the absorption properties of a birefringent material. Loss tangents for light polarized along the fast and slow axis are generally different. The result is a modulated signal that appears at twice the rotational frequency of the birefringent plate. For the dual Martin-Puplett modulator, there are two important effects to consider. First, for different settings of the translational stage, the illumination will potentially change, thereby introducing a spurious polarization signal. This problem can be avoided by restricting the use of such modulators to slow optical systems in which the beam growth through the modulator is minimal. The second concern involves the differential absorption of the grids and the mirrors of the modulator. For the rooftop mirrors, the incident angle of the radiation is the same for different modulator positions. Thus, the Fresnel coefficients for each of the two polarizations will remain essentially constant during the modulation process.

7. Use as a Calibrator

In the laboratory, the ability of these devices to work at room temperature may make them excellent calibrators. An input polarized signal can be transformed quite easily to test the polarization response of a precision polarization sensor. It can transform an initially linearly polarized state into an elliptical polarization state.

8. Experimental Results

8.A. Setup

To test the concept of polarization modulation using phase control, we built the Martin-Puplett interferometer configuration illustrated in Figure 2. The beam exiting the horn

attached to port 1 is collimated by an ellipsoidal mirror. It then passes through a polarizing grid that has its wires oriented at a 45° angle in projection. Each orthogonal polarization is then launched down a separate arm of the interferometer and reflects off of a rooftop mirror which rotates the polarization vector by 90°. The beams recombine at the polarizer and are refocused into the feed connected to port 2. The setup is symmetric, and so, the reverse light path is identical. The rooftop mirrors are placed on translational stages, such that their relative distance can be adjusted. The frequency-dependent phase that corresponds to this path length differential is the parameter that determines the mapping between polarization states on either end of the device.

This quasioptical setup is a 4-port device with the 2 ports on either end of the device being defined by the vertically (V) and horizontally (H) polarized electric field modes. We use an Hewlett Packard HP8106D millimeter wave vector network analyzer (VNA) to measure the scattering parameters between these modes. The calibration reference plane is shown (Γ_1 and Γ_2) in Figure 2. The VNA can be used to measure the 2×2 scattering matrices of pairs of these ports, so in order to reduce contamination of our results, we place an orthomode transducer(OMT)[14] at the back of each feedhorn and terminate the unused polarization with a matched load. For the purposes of these measurements, it is useful to think of the end of the quasioptical device attached to port 1 of the VNA as the source and that attached to port 2 as the detector. We set the polarization state of the source to be vertically-polarized light (a pure Q state) by orienting the waveguide appropriately. On the detector side, we measure both V and H in successive measurements by respectively omitting and adding a 90° twist to the WR-10 waveguide between the OMT and the Γ_2 calibration point. The calibrated difference between the power associated with H and V gives a measurement of Stokes Q at the detector. We have measured the loss of the twist to be 0.15 dB.

The bandwidth of the test setup is approximately 78-115 GHz. At the low end of the band, the band edge is defined by that of the W-band feed horns, and at the high end, it is defined by the OMT return loss.

8.B. Experimental Procedure

We found the zero path length position by first maximizing the signal in the V direction at a point where the S_{21} parameter was flat across the band. We then were able to use the first null condition to do a fine adjustment. V and H are measured for 27 combinations of positions of the two mirrors having path differences corresponding to 24° steps in phase for λ= 3 mm. Four sample spectra are shown in Figure 3. We have included in these plots the expected spectra ($H \propto \sqrt{1 - \cos \Delta}$ and $V \propto \sqrt{1 + \cos \Delta}$), adopting a global gain of 0.9 dB to account for the expected loss beyond the calibration port. The return loss of the system is about 13 dB and can be seen in the H component of Figure 3A. The transmission efficiency

of the horns is not constant across the band and tends to roll off at low frequencies.

8.C. Results

This experimental setup is described mathematically by the expression in Equation 21. In this case,

$$Q_{det} = \frac{H(\Delta)^2 - fV(\Delta)^2}{H(\Delta)^2 + fV(\Delta)^2} = Q_{source} \cos \Delta + V_{source} \sin \Delta \qquad (26)$$

where $\Delta = 4\pi(d_2 - d_1)/\lambda$. Here, $H(\Delta)^2$ and $V(\Delta)^2$ are the powers corresponding to S_{21} when the twist is included and excluded, respectively. For each frequency, the relative gain factor, f, is calculated by fitting for the average values of the signals in the H and V configurations and taking the ratio.

For every frequency, it is possible to measure Stokes Q and V. The result of this fit is shown in Figure 4. We find that the average Stokes parameters measured over the 78-115 GHz band are $Q = -1.002 \pm 0.003$ and $V = 0.001 \pm 0.013$. There is some non-zero power in Stokes V near the high end of the band. It is unclear as to whether this is due to a systematic effect or due to an unknown source polarization.

8.D. Resonances

In this laboratory setup, proper termination of the unused port at both the entrance and exit apertures is essential, as even small reflections can introduce resonances. These resonances are an indication of the level of uncertainty of phase control of the radiation propagating through the interferometer. This uncertainty directly leads to a frequency-dependent random mixing between the Q and V polarization states and hence a decrease in the precision of the Martin-Puplett interferometer as a polarimeter. We have found that this systematic "noise" can be controlled by various levels of termination of the unused polarization. The addition of the OMTs in the signal chain reduced the noise in the S_{21} parameter from 3 dB to 1 dB. We also added a horizontal grid at the mouth of the source feedhorn to redirect any residual H component to an eccosorb beam dump. This grid reduced the noise in S_{21} to 0.25 dB and also reduced the average coupling of Q into V from 4% to under 1%.

On a telescope, this problem is mollified by the fact that the source port is nearly perfectly terminated on the sky. This greatly reduces phase uncertainties in the system as well as the need for excessive polarization filtering.

9. Summary

We have described a new technique for polarization modulation and calibration applicable from the far-infrared through millimeter parts of the electromagnetic spectrum. In the far-infrared through submillimeter where bandpasses are typically $\Delta\lambda/\lambda \sim 0.1$, this device can be used in a similar manner to a half-wave plate. Broader bandpasses ($\Delta\lambda/\lambda \sim 0.3$) may be accommodated using more complex modulation schemes. In the millimeter, this device may find use as a partially-polarized calibration source. The Martin-Puplett architecture provides a modulator that can be made robust, broadband, and easily tunable to different wavelengths. In addition, it allows for the complete determination of the polarization state of the incoming radiation by the measurement of Stokes Q, U, and V.

Acknowledgments

References

1. W. S. Holland, W. Duncan, B. D. Kelly, K. D. Irwin, A. J. Walton, P. A. R. Ade, and E. I. Robson, "SCUBA-2: a new generation submillimeter imager for the James Clerk Maxwell Telescope," in *Millimeter and Submillimeter Detectors for Astronomy. Edited by Phillips, Thomas G.; Zmuidzinas, Jonas. Proceedings of the SPIE, Volume 4855, pp. 1-18 (2003).*, pp. 1–18 (2003).

2. D. A. Harper, A. E. Bartels, S. C. Casey, D. T. Chuss, J. L. Dotson, R. Evans, S. Heimsath, R. A. Hirsch, S. Knudsen, R. F. Loewenstein, S. H. Moseley, M. Newcomb, R. J. Pernic, T. S. Rennick, E. Sandberg, D. B. Sandford, M. L. Savage, R. F. Silverberg, R. Spotz, G. M. Voellmer, P. W. Waltz, S. Wang, and C. Wirth, "Development of the HAWC far-infrared camera for SOFIA," in *UV and Gamma-Ray Space Telescope Systems. Edited by Hasinger, Günther; Turner, Martin J. L. Proceedings of the SPIE, Volume 5492, pp. 1064-1073 (2004).*, pp. 1064–1073 (2004).

3. J. Tinbergen, *Astronomical Polarimetry* (Cambridge, 1996).

4. R. H. Hildebrand, J. A. Davidson, J. L. Dotson, C. D. Dowell, G. Novak, and J. E. Vaillancourt, "A Primer on Far-Infrared Polarimetry," PASP **112**, 1215–1235 (2000).

5. E. Battistelli, M. DePetris, L. Lamagna, R. Maoli, F. Melchiorri, E. Palladino, and G. Savini, "Far infrared polarimeter with very Low Instrumental Polarization," astro-ph/0209180v1 (2002).

6. B. R. Johnson, M. E. Abroe, P. Ade, J. Bock, J. Borrill, J. S. Collins, P. Ferreira, S. Hanany, A. H. Jaffe, T. Jones, A. T. Lee, L. Levinson, T. Matsumura, B. Rabii, T. Renbarger, P. L. Richards, G. F. Smoot, R. Stompor, H. T. Tran, and C. D. Winant, "MAXIPOL: a balloon-borne experiment for measuring the polarization anisotropy of the cosmic microwave background radiation," New Astronomy Review **47**, 1067–1075 (2003).

7. R. Jones, "New Calculus for the Treatment of Optical Systems," J. Opt. Soc. Am. **31**, 488–493 (1941).

8. C. Brosseau, *Fundamentals of Polarized Light* (Wiley, 1998).

9. J. Jackson, *Classical Electrodynamics* (Wiley, 1967).

10. D. E. Budil, Z. Ding, G. R. Smith, and K. A. Earle, "Jones Matrix Formalism for Quasioptical EPR," Journal of Magnetic Resonance **144**, 20–34 (2000).

11. S. Sternberg, *Group Theory and Physics* (Cambridge, 1994).

12. G. Siringo, E. Kreysa, L. A. Reichertz, and K. M. Menten, "A new polarimeter for (sub)millimeter bolometer arrays," å**422**, 751–760 (2004).

13. T. Manabe, J. Inatani, A. Murk, R. J. Wylde, M. Seta, and D. H. Martin, "A New Configuration of Polarization-Rotating Dual-Beam Interferometer for Space Use," IEEE Transactions on Microwave Theory and Techniques **51**(6), 1696–1704 (2003).

14. E. Wollack and W. Grammer, "Symmetric Waveguide Orthomode Junctions," in *Proceedings of the 14th International Symposium on Space TeraHertz Technology*, E. Walker and J. Payne, eds., pp. 169–176 (2003).

Table 1. A summary of physical transformation of optical elements, their Jones matrix representations, and their Pauli algebra representations are given.[10] For the linear distance transformation, d represents the distance traveled. For the mirror, a rotation of the mirror has no effect, and thus $\bar{Q}$ is a general representation for this element. For the wire grid, θ is the angle of the grid wires with respect to the $\hat{H}$-axis. For the rooftop mirror, θ is the angle between the roofline and the $\hat{H}$-axis. For the birefringent plate, θ is the angle between the fast axis of birefringence and the $\hat{H}$-axis, and ξ is half of the phase delay introduced between the orthogonal polarizations.

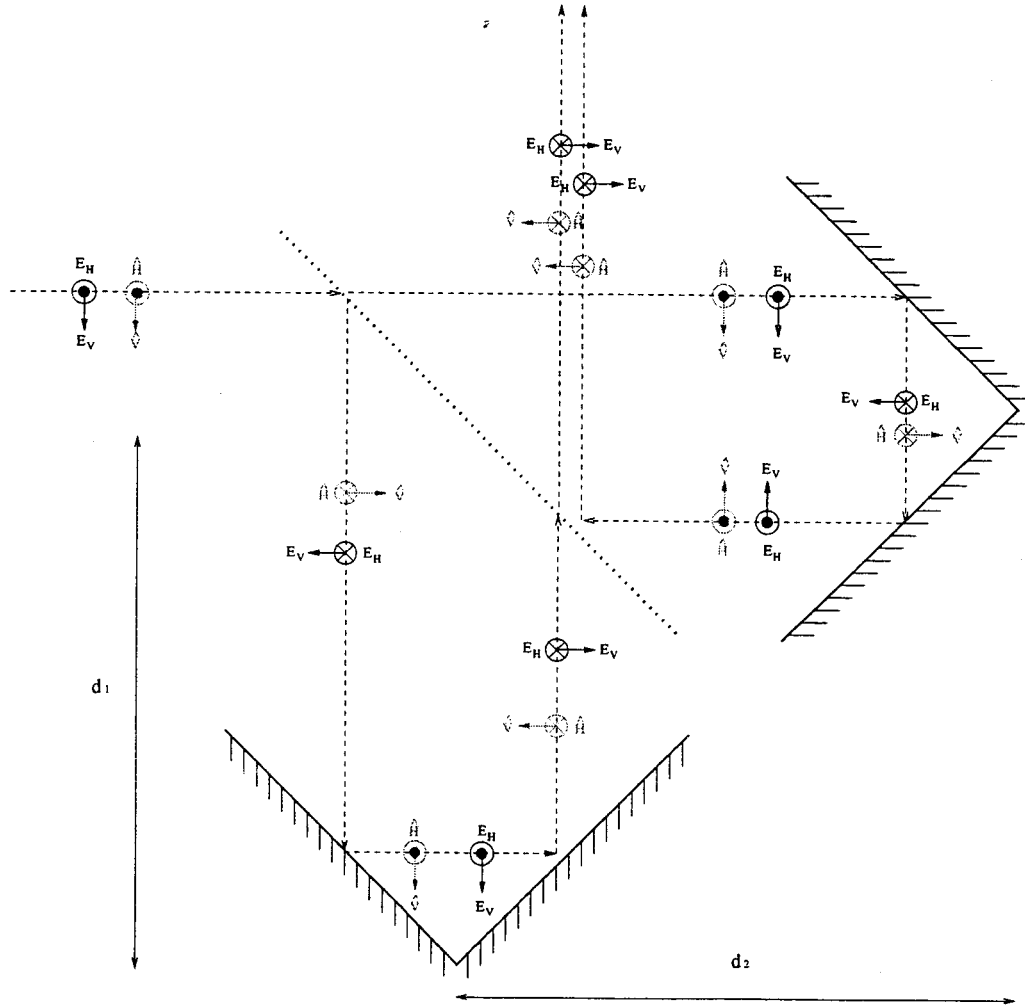| Description	Symbol	Matrix Representation	Stokes Expansion
Linear Distance	$\bar{J}_z(d)$	$\begin{pmatrix} \exp(i2\pi d/\lambda) & 0 \\ 0 & \exp(i2\pi d/\lambda) \end{pmatrix}$	$\bar{I}\exp(i2\pi d/\lambda)$
Mirror	$\bar{J}_M$	$\begin{pmatrix} 1 & 0 \\ 0 & -1 \end{pmatrix}$	$\bar{Q}$
Wire grid (ref.)	$\bar{J}_{WR}(\theta)$	$\begin{pmatrix} \cos^2\theta & \sin\theta\cos\theta \\ -\sin\theta\cos\theta & -\sin^2\theta \end{pmatrix}$	$\frac{1}{2}(\bar{Q} + \bar{I}\cos 2\theta + i\bar{V}\sin 2\theta)$
Wire grid (trans.)	$\bar{J}_{WT}(\theta)$	$\begin{pmatrix} \sin^2\theta & -\sin\theta\cos\theta \\ -\sin\theta\cos\theta & \cos^2\theta \end{pmatrix}$	$\frac{1}{2}(\bar{I} - \bar{Q}\cos 2\theta - \bar{U}\sin 2\theta)$
Coord. rotation	$\bar{R}(\theta)$	$\begin{pmatrix} \cos\theta & \sin\theta \\ -\sin\theta & \cos\theta \end{pmatrix}$	$\bar{I}\cos\theta + i\bar{V}\sin\theta$
Rooftop mirror	$\bar{J}_{RT}$	$\begin{pmatrix} \cos 2\theta & \sin 2\theta \\ \sin 2\theta & \cos 2\theta \end{pmatrix}$	$\bar{I}\cos 2\theta + i\bar{V}\sin 2\theta$
Birefringent plate	$\bar{J}_{WP}(\theta,\xi)$	$\begin{pmatrix} \cos\xi - i\sin\xi\cos 2\theta & -i\sin\xi\sin 2\theta \\ -i\sin\xi\sin 2\theta & \cos\xi + i\sin\xi\cos 2\theta \end{pmatrix}$	$\bar{I}\cos\xi - i\sin\xi(\bar{Q}\cos 2\theta + \bar{U}\sin 2\theta)$

Fig. 1. The propagation of the electric field components and the $(\hat{H}, \hat{V})$ co-ordinate axes through a Martin-Puplett interferometer at an angle of $\pi/4$ are shown. When $d_1 = d_2$, this device behaves like a mirror. When there is a path difference, it changes the polarization state of the incoming radiation.

Table 2. The mapping of Q_{det} onto the sky for selected values of Δ_1 and Δ_2 for dual modulators is given. In this case, $\theta_1 = \pi/8$ and $\theta_2 = \pi/4$.

Δ_1	Δ_2	Q_{det}
0	0	Q_{sky}
0	π	$-Q_{sky}$
π	0	U_{sky}
π	π	$-U_{sky}$
0	$\pi/2$	$-V_{sky}$
$\pi/2$	0	$\frac{1}{2}(Q_{sky} + U_{sky}) + \frac{1}{\sqrt{2}}V_{sky}$
$\pi/2$	π	$-\frac{1}{2}(Q_{sky} + U_{sky}) - \frac{1}{\sqrt{2}}V_{sky}$
π	$\pi/2$	V_{sky}
$\pi/2$	$\pi/2$	$\frac{1}{\sqrt{2}}(Q_{sky} + U_{sky})$

To VNA Port 2 →

90 degree twist
(added for H →
measurements)

Γ_2

OMT 2

W–Band Feeds (corrugated)

Rooftop Mirror1

Rooftop Mirror 2

Polarizing Grid
(wires at 45°)

Γ_1

OMT 1

To VNA Port 1

Polarizing Grid
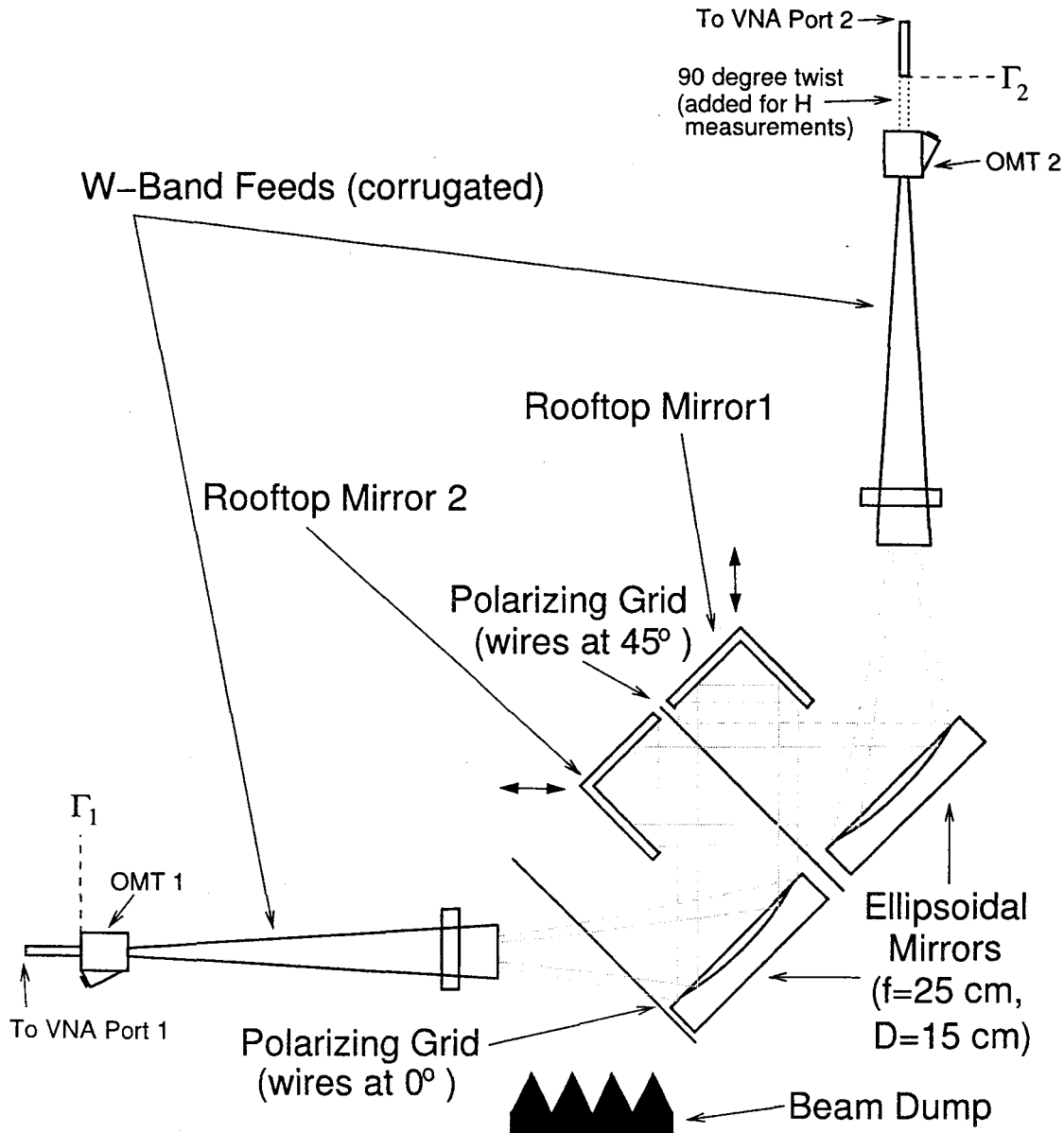(wires at 0°)

Ellipsoidal
Mirrors
(f=25 cm,
D=15 cm)

Beam Dump

Fig. 2. The modified Martin-Puplett interferometer is symmetrically fed by a pair of W-Band feed horns (25-27 dBi) that are collimated by ellipsoidal mirrors (f=25 cm). Each of the two rooftop mirrors reflect a component of polarizations. The mirrors are mounted on transports that are used to adjust the path lengths of the individual polarizations. The polarizing grid is mounted such that the wires make an angle of 45° with the roof lines in projection. The dashed and dotted lines show the positions of the beam radius (8.7 dB edge taper) and 20 dB edge taper, respectively, of a Gaussian beam propagating through the structure for a 26 dBi feed and a wavelength of 3 mm (100 GHz). We have illustrated the location of the 90° twist on port 2 that converts the sensitivity of port 2 from V to H. The calibration reference plane is also shown (Γ_1 and Γ_2.)
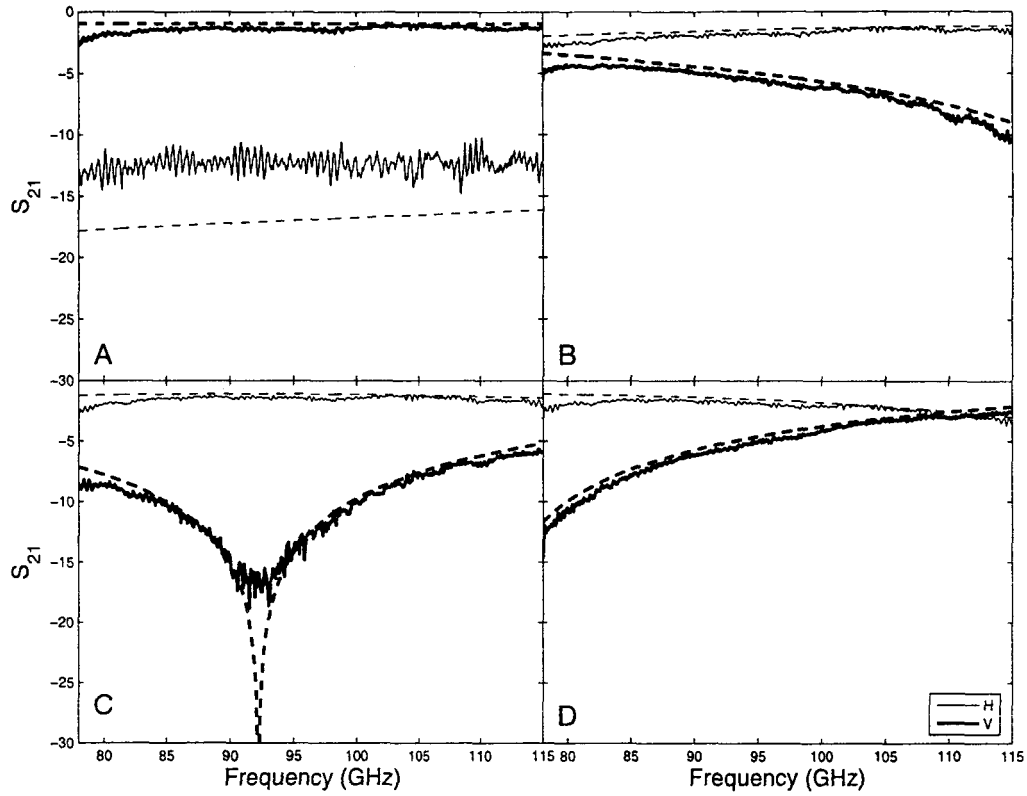
Fig. 3. The output spectra are shown for four different values of $d_1 - d_2$: (A) -13 μm, (B) 587 μm, (C) -813 μm, and (D) -1013 μm. The red solid line is the spectrum of the V linear polarization measured at port 2 of the VNA. The blue solid line in each plot is the spectrum of the H linear polarization measured at port 2. The H polarization is measured by adding a 90° twist in the WR-10 waveguide attached to port 2 of the VNA. Theoretical predictions for H and V are plotted as blue and red dashed lines, respectively.
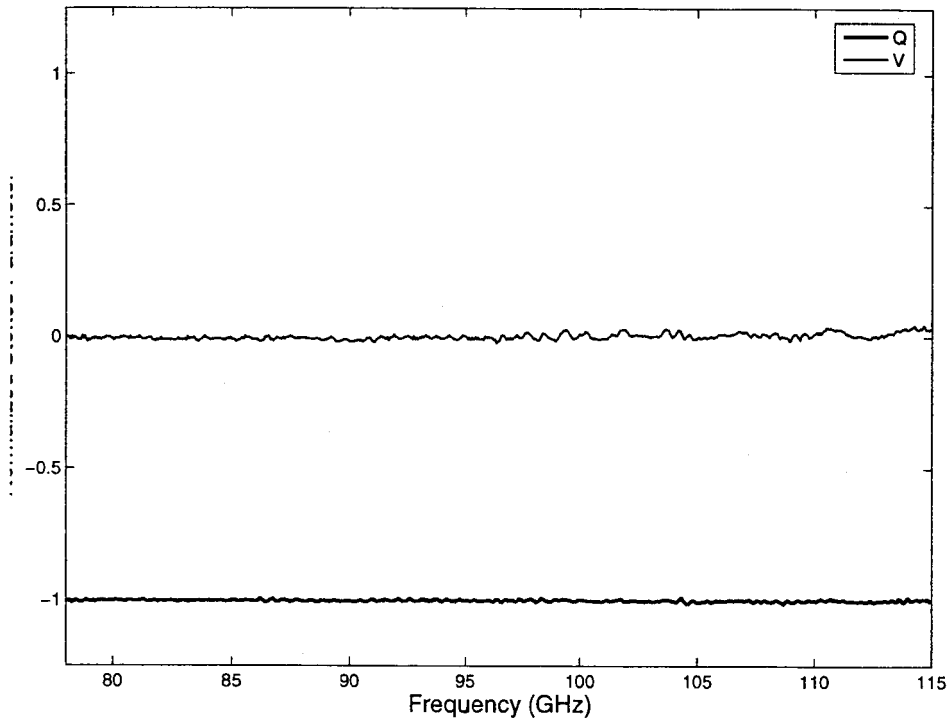
Fig. 4. The normalized Stokes parameters q and v are calculated as a function of frequency by fitting to the 16 mirror positions. The mean values of q and v across the 78-115 GHz band are -1.002±0.003 and 0.001±0.013, respectively.